Research Journal of Applied Sciences, Engineering and Technology 7(1): 150-156, 2014
DOI:10.19026/rjaset.7.232
ISSN: 2040-7459; e-ISSN: 2040-7467

Submitted: March 06, 2013 Accepted: April 02, 2013 Published: January 01, 2014

Research Article

Influences of Cylindrical Carrier's Size and Shape of Undersurface on the Directivity of Vector Sensor

Liang Guo-Long, Pang Fu-Bin and Zhang Guang-Pu
National Laboratory of Underwater Acoustic Technology, Harbin Engineering University, Harbin 150001, China

Abstract: When the acoustic vector sensor is installed on underwater carrier to detect and position targets, the measuring results will be influenced by the diffraction of the carrier. Due to the differences of the sizes and shapes of the carrier, the influences of the diffraction on acoustic vector sensor are also different. Using BEM, the influences of cylinder's size and shape of undersurface on the directivity of acoustic vector sensor are calculated in this study. The results show that: the influences of diffraction on acoustic vector sensor are proportional to the length of cylinder's radius and height; besides, the sharper the undersurface is, the less influences acoustic vector sensor subjects to diffraction of the carrier. The experiment that carried out in the lake proves the validity of the computing. The research is effective guidance for the application of acoustic vector sensor.

Keywords: Acoustic vector sensor, cylindrical carrier, directivity, size and shape of undersurface

INTRODUCTION

Composed by omni directional sound pressure sensor and dipole directional particle velocity sensor, acoustic vector sensors picks up both pressure and vibration velocity information in acoustic field, which expends the signal processing space and provides new thought and method for solving underwater acoustic problems (Sun and Li, 2004). However, when it is installed on underwater carrier to detect and position targets, the diffraction of the carrier will distort the free space field, thus influencing the measuring results of vector sensor. To find out how the carrier's size and shape of undersurface affects the directivity of vector sensor and further select the reasonable carrier to reduce the diffraction, is very meaningful for the application of vector sensor.

In recent decades, the diffraction characteristics of objects in shape of sphere, cylinder and et al. have been studied by scholars home and abroad. The pressure and velocity of acoustic diffraction field by infinite rigid spheroid have been calculated using MATLAB PDE toolbox and the method of calculating the diffraction of shell structure in any shape is proposed (Kang, 2002). Systematic research on signal processing of acoustic vector sensor by a reflecting boundary has been carried out (Malcolm and Arye, 2000). The theory of resonance radiation of submerged elastic spherical and cylindrical shell have been studied (Tang and Fan, 2000; Liu *et al*., 2002). The mathematical expressions of pressure and velocity in diffraction field by prolate spheroid are deduced and the experimental results coincide well with the theoretical results (Ji *et al*., 2010). The model of the diffraction by elastic shell with filler inside using BEM+FEM is built and the calculating results show that the diffraction of the filler will change the characteristics of acoustic field (Zhuo *et al*., 2009). In this study, the influences of cylindrical carrier's sizes, shapes of undersurface on the directivity of acoustic vector sensor are studied and experiment was carried out to prove the validity of the calculation.

THEORY OF DIFFRACTION CALCULATION USING BEM

The wave propagating equation under single frequency can be guided to Helmholtz equation. As

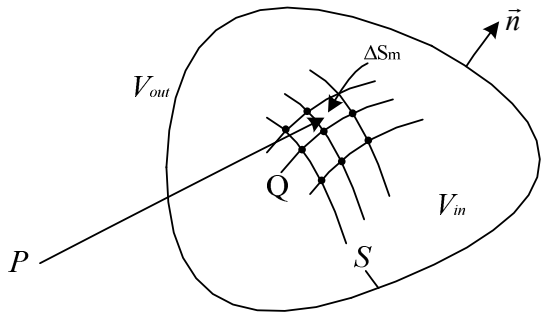

Fig. 1: Schematic diagram of exterior acoustic problem

Corresponding Author: Liang Guo-Long, National Laboratory of Underwater Acoustic Technology, Harbin Engineering University, Harbin 150001, China

shown in Fig. 1, the enclosed vibrating body V locates in infinite fluid mass whose density sound velocity are ρ and c respectively. P is a point in the space and the Helmholtz equation in exterior field is expressed as (Шендеров *et al*., 1983):

$$\nabla^2 p(P) + k^2 p(P) = 0 \quad (1)$$

where,

$k = w/c$ = The wave number of the incident wave
Q = A point on surface S
$\vec{n}$ = The exterior normal direction of the vibrating body

The integral equation of pressure at point P in sound field can be expressed as (He and Zhao, 1992):

$$\alpha p(P) = \iint_S (p(Q)\frac{\partial G(P,Q)}{\partial \vec{n}} - \frac{\partial p(Q)}{\partial \vec{n}} G(P,Q))dS \quad (2)$$

where, $\alpha = 4\pi$, when $P \in V_{out}$(outside surface S); $\alpha = 2\pi$, when $P \in S$; $\alpha = 0$, when $P \in V_{in}$(inside surface S). G is the three-dimensional Green function in free space and it satisfies the equation as follows:

$$\nabla^2 G(P,Q) + k^2 G(P,Q) = -\delta(P,Q), \quad \delta(P,Q) = \begin{cases} 0 & P \neq Q \\ \infty & P = Q \end{cases} \quad (3)$$

Utilizing the Euler equation, the pressure $p(Q)$ and normal velocity $u(Q)$ on surface S can be deduced as:

$$\frac{\partial p(Q)}{\partial \vec{n}} = -j\rho ck u(Q) \quad (4)$$

By introducing Formula (4) into Formula (2), the pressure of point P can be obtained as:

$$\alpha p(P) = \iint_S (p(Q)\frac{\partial G(P,Q)}{\partial \vec{n}} + j\rho ck u(Q) G(P,Q))dS \quad (5)$$

From Formula (5), it can be indicated that if vibration velocity and pressure on surface S are known parameters, then the pressure of any point in exterior field can be calculated. However, limited to the measuring conditions and the complicated shape of the surface, vibration velocity and pressure information usually can't be both obtained. According to BEM theory, surface S can be divided into many small elements named ΔS_m. Then the integration form of Formula (5) is converted into the summing of each small element. Assume the pressure and velocity of any point in element ΔS_m are expressed with the pressure p_m^l and velocity u_m^l of the nodes as follows:

$$p_m(\zeta,\eta) = \sum_{l=1}^{L} N_l(\zeta,\eta)\, p_m^l \quad (6)$$

$$u_m(\zeta,\eta) = \sum_{l=1}^{L} N_l(\zeta,\eta)\, u_m^l \quad (7)$$

where,

N_l = The interpolation function of the element
(ζ,η) = The local coordinate of the point in the element

The transforming relationship between main and local coordinates is Jacobi Factor $J(\zeta,\eta)$, whose expression is:

$$J(\zeta,\eta) = \begin{vmatrix} i & j & k \\ \frac{\partial x}{\partial \zeta} & \frac{\partial y}{\partial \zeta} & \frac{\partial z}{\partial \zeta} \\ \frac{\partial x}{\partial \eta} & \frac{\partial y}{\partial \eta} & \frac{\partial z}{\partial \eta} \end{vmatrix} \quad (8)$$

Assume that the number of the elements is M. By introducing Formula (6), (7) into Formula (5), the interpolation function can be converted into algebraic function as follows:

$$\alpha p(P) = \sum_{m=1}^{M} \iint_{\Delta S_m} \frac{\partial G}{\partial \vec{n}} |J(\zeta,\eta)| \sum_{l=1}^{L} N_l(\zeta,\eta)\, p_m^l dS_m(\zeta,\eta) + \sum_{m=1}^{M} \iint_{\Delta S_m} j\rho ckG|J(\zeta,\eta)| \sum_{l=1}^{L} N_l(\zeta,\eta)\, u_m^l dS_m(\zeta,\eta) \quad (9)$$

If there are T nodes on surface S and the column matrix of the pressure and velocity of the nodes are:

$$\begin{cases} [p_s] = [p_1, p_2, \ldots \ldots p_T] \\ [u_s] = [u_1, u_2, \ldots \ldots u_T] \end{cases} \quad (10)$$

By introducing Formula (10) into Formula (9), the matrix expression of Formula (9) can be obtained as follows:

$$\alpha p(P) = [A][p_s] + [B][u_s] \quad (11)$$

where,

$$A = \sum_{m=1}^{M} \iint_{\Delta S_m} \frac{\partial G}{\partial \vec{n}} |J(\zeta,\eta)| NK dS_m(\zeta,\eta) \quad (12)$$

$$B = \sum_{m=1}^{M} \iint_{\Delta S_m} j\rho ckG|J(\zeta,\eta)| NK dS_m(\zeta,\eta) \quad (13)$$

and N is the interpolation matrix as follows

$$N = [N_1(\zeta,\eta), N_2(\zeta,\eta), \ldots \ldots N_L(\zeta,\eta)]_{1\times L} \quad (14)$$

K is the transforming matrix between element nodes' degree of freedom and structure nodes' degree of freedom:

$$K = \begin{bmatrix} 0 & 0 & 0 & \cdots & 1 & 0 \\ \vdots & 1 & 0 & \cdots & 0 & \vdots \\ \vdots & \vdots & \vdots & \cdots & \vdots & 1 \\ 0 & 0 & 1 & \cdots & 0 & 0 \end{bmatrix}_{L\times T} \quad (15)$$

When observing point P is outside surface S,

$$4\pi p(P) = [A][p_s] + [B][u_s] \quad (16)$$

When observing point P is on surface S,

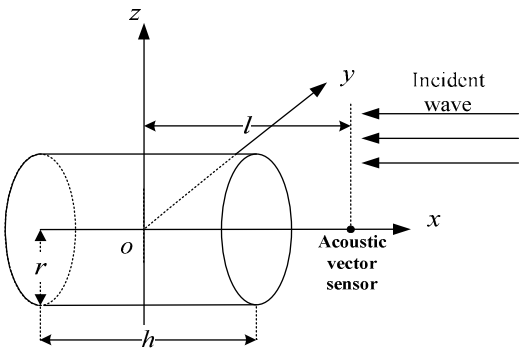

Fig. 2: Schematic diagram of position relation between acoustic vector sensor and cylinder

Table 1: Parameters of carrier models with different radiuses and heights

	Model 1	Model 2	Model 3
r	0.1 m	0.2 m	0.1 m
h	0.5 m	0.5 m	0.25 m
l	0.4 m	0.4 m	0.4 m

$$2\pi p(P) = [A][p_s] + [B][u_s] \quad (17)$$

Utilizing Formula (17), the value of pressure and vibration velocity of any point on surface S can be obtained if either of them is known. By taking the value of pressure and vibration velocity of the surface into Formula (16), the sound field of any point outside the surface can be calculated.

SIMULATION AND ANALYSIS

Calculating model: As shown in Fig. 2, the radius of the cylinder is r and the height is h. Acoustic vector sensor locates l away from the center of the carrier on the positive x axis. The vertical and horizontal vibration velocity of the sensor points along the positive x, y axis.

The mass density and sound velocity of the cylinder are 7850 kg/m^3 and 5100 m/s respectively. The carrier is placed in quiescent, isotropic, homogeneous, infinite fluid water, whose mass density is 1000 kg/m^3 and sound velocity is 1500 m/s. When the incident plane wave is along the negative x axis, the incident angle is defined as 0°. The influences of diffraction by the carrier on the directivity of acoustic vector sensor will be calculated as the incident wave rotates a circle around the origin.

Carriers with different radiuses and heights: The parameters of models with different radiuses and heights are shown in Table 1. Model 1 is the model for comparison, whose radius is 0.1 m and height is 0.4 m. The radius of model 2 is twice as large as model 1 and the height of model 3 is half as large as model 1. The distance from acoustic vector sensor and the center of the carrier is 0.4 m for all the models.

The influences of the diffraction by three models on the directivity of acoustic vector sensor are shown in Fig. 3. At 300 Hz, the amplitude of diffraction wave is small and the directivity of pressure is close to natural free field directivity. However, though the directivity of vertical and horizontal vibration velocity are still dipole, the amplitude of both channels has changed. Figure 3b illustrates the influences of the diffraction by three models on the directivity of vertical vibration velocity at different frequencies. Obviously the influences of diffraction by model 3 are the least and the influences of diffraction by model 1 are less, while the influences of diffraction by model 2 are the most of the three. With the increasing of incident frequency, the diffraction wave by the models grows larger and the directivity of all channels becomes worse. At 2500 Hz, the directivity of vertical vibration velocity by the diffraction of model 2 has seriously deviated from dipole directivity.

Combing with the parameters of Table 1, it can be inferred that the influences of diffraction by the models are proportional to the length of cylinder's radius and heights. Besides, the directivity of pressure and vibration velocity of the sensor by the diffraction of model 1 is better than that of model 2, which implies that influences from the radius are larger than that from the height.

Carriers with different shapes of undersurface: The schematic diagram of models with different shapes of undersurfaces is shown in Fig. 4. The height and radius of all the models are h and r respectively. All three models are fixed with different shapes of undersurface whose heights are h_1. Acoustic vector sensor still locates l away from the center of the carrier and the parameters of three models are shown in Table 2.

The influences of the diffraction by three models on the directivity of acoustic vector sensor are shown in Fig. 5. The directivity of pressure and horizontal vibration velocity is less influenced by the diffraction, while the directivity of vertical vibration velocity is seriously distorted at different incident frequencies. This is because the intensity of diffraction wave concentrates in the x axis direction. From Fig. 5b, it can be inferred that the influences of diffraction by model 6 are the least and the influences of diffraction by model 5are less, while the influences of diffraction by model 4 are the most of all.

From Table 2 it can be inferred that the sharper the shape of the undersurface is, the less influences acoustic vector sensor subjects to the diffraction by the carrier. When the undersurface is sharp, the intensity of diffraction wave diffuses all directions and little is picked up by acoustic vector sensor, which makes its directivity close to natural free field directivity.

EXPERIMENTAL RESULTS AND ANALYSIS

The experiment of influences on the directivity of acoustic vector sensor by cylindrical carrier was carried

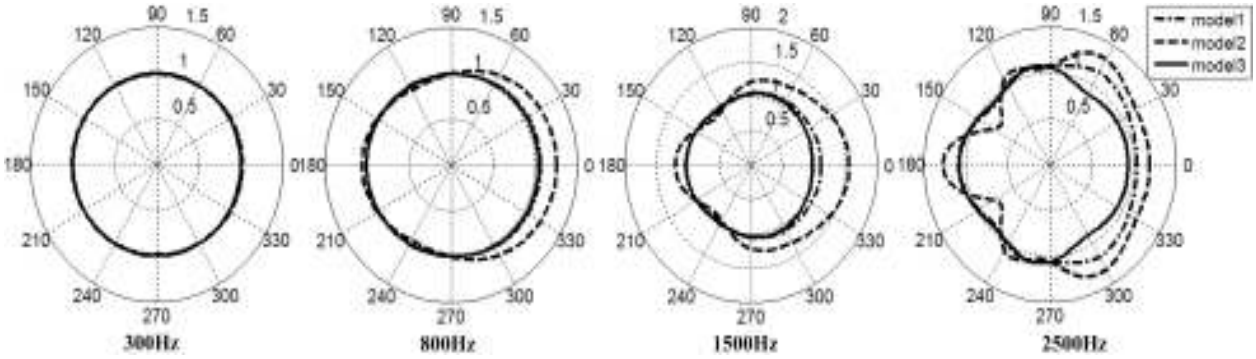

(a) pressure

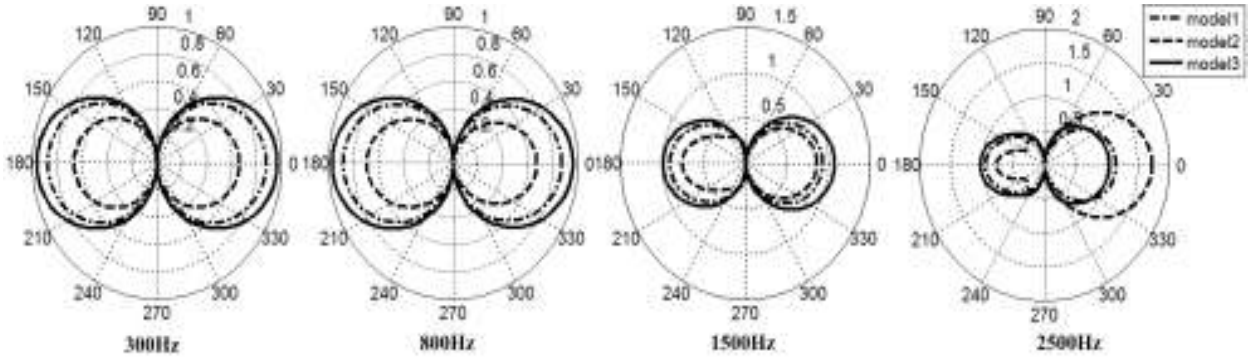

(b) vertical vibration velocity (in *x* axis)

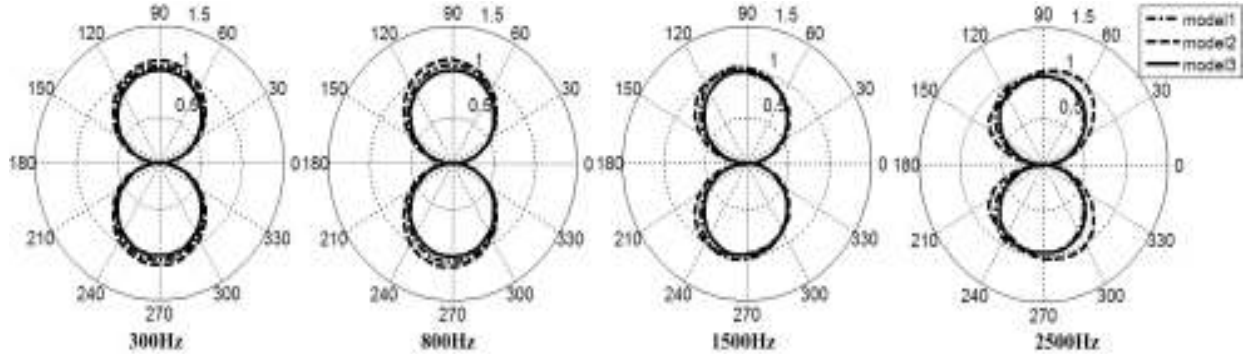

(c) horizontal vibration velocity (in *y* axis)

Fig. 3: Directivity of acoustic vector sensor by the diffraction of models in Table 1

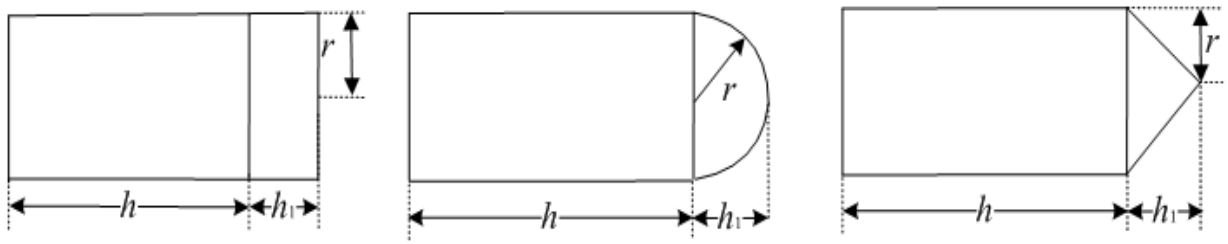

(a) model4 (b) model5 (c) model6

Fig. 4: Schematic diagram of models with different shapes of undersurface

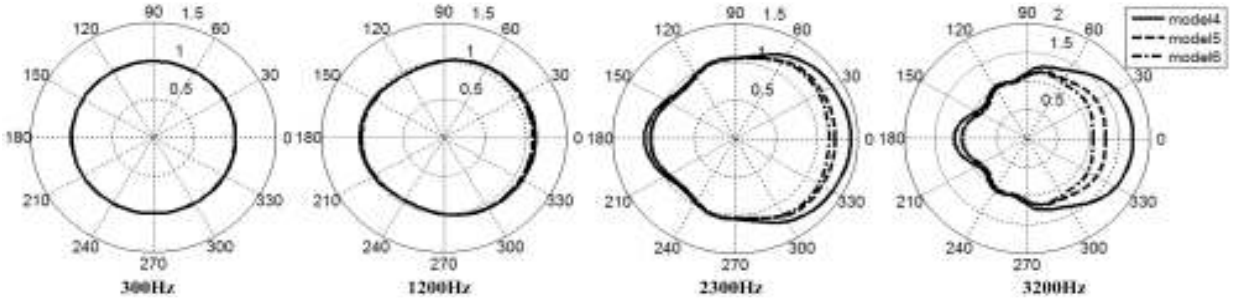

(a) pressure

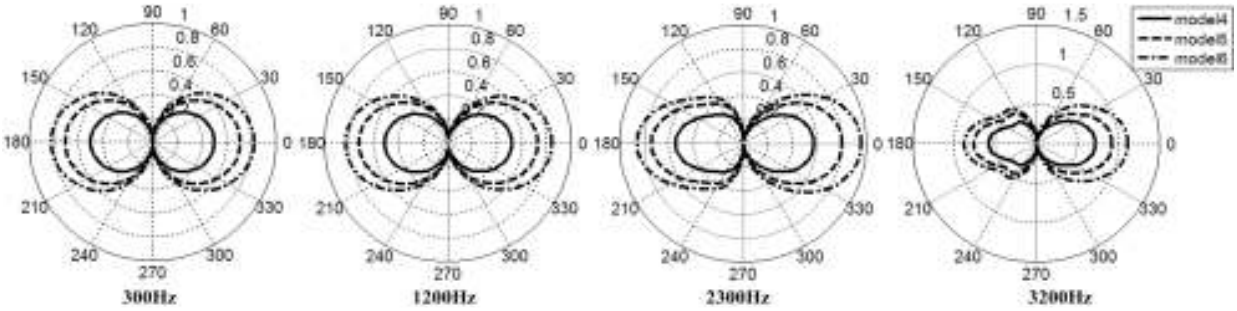

(b) vertical vibration velocity (in *x* axis)

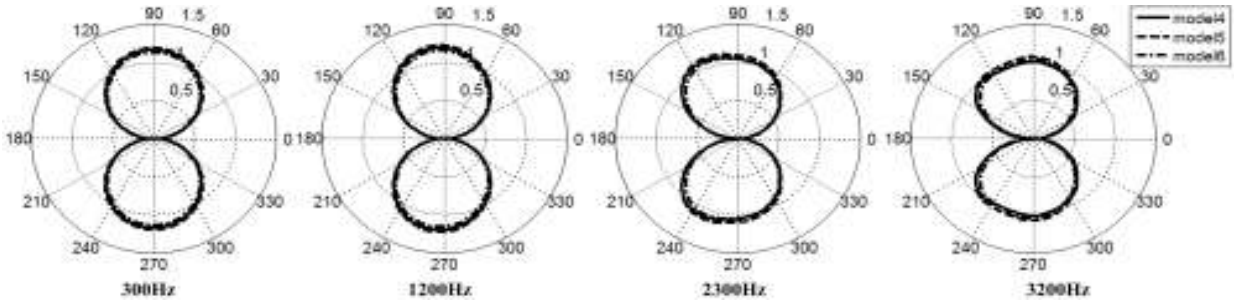

(c) horizontal vibration velocity (in *y* axis)

Fig. 5: Directivity of acoustic vector sensor by the diffraction of models in Table 2

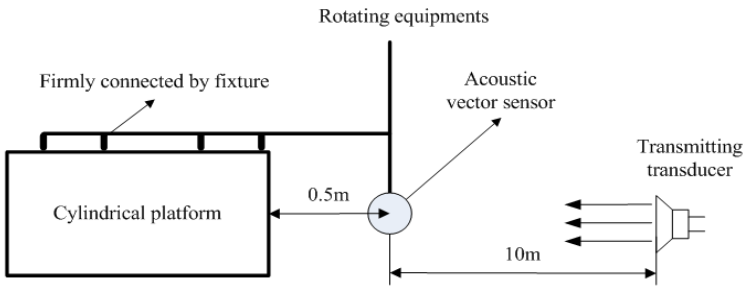

Fig. 6: Schematic diagram of experimental model

Table 2: Parameters of models with different shapes of undersurface

	Model 4	Model 5	Model 6
r	0.1 m	0.1 m	0.1 m
h	0.5 m	0.5 m	0.5 m
h_1	0.1 m	0.1 m	0.1 m
l	0.4 m	0.4 m	0.4 m
Shape	Plane	Hemispherical	Conical

out in the lake and the experimental model is shown in Fig. 6. Acoustic vector sensor is fixed 0.5 m away from center of the carrier. The transmitting transducer is 10m away from the sensor and the incident wave is approximated as plane wave. Due to the restriction of the experimental condition, the cylindrical carrier is

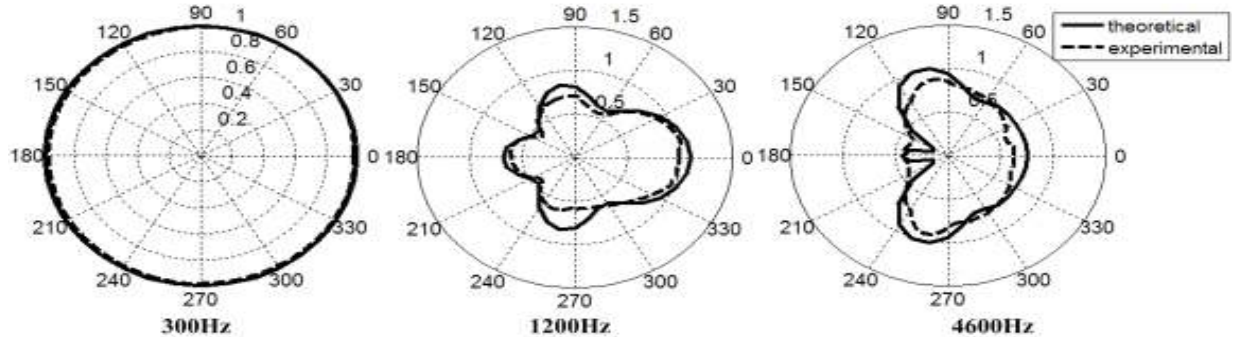

(a) pressure

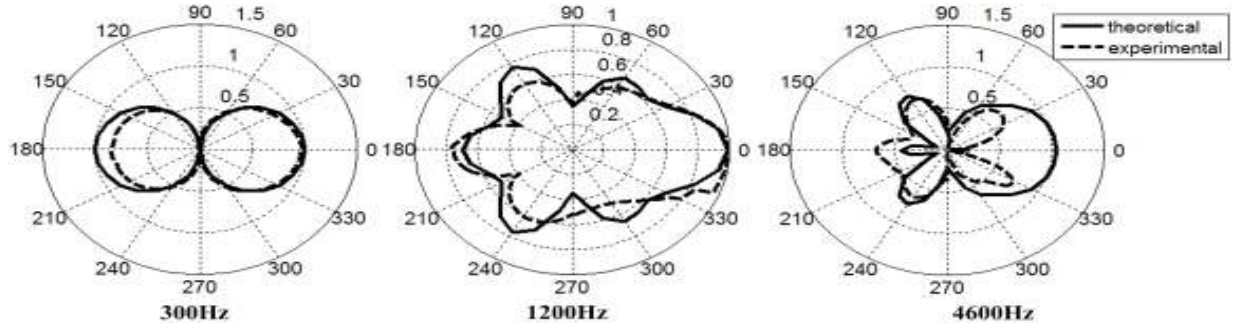

(b) vertical vibration velocity (in *x* axis)

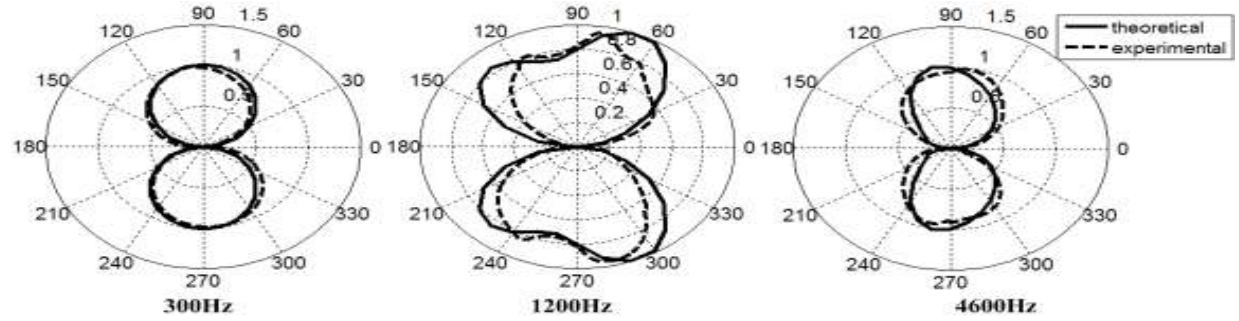

(c) horizontal vibration velocity (in *y* axis)

Fig. 7: Comparison of theoretical and experimental results

chosen as a closed cylinder shell with air inside and water outside, whose mass density and sound velocity are 1.29 kg/m^3, 1000 kg/m^3 and 340 m/s, 1500 m/s respectively. The material of the carrier shell is steel, whose density is 7850 kg/m^3, Poisson ratio is 0.28, Young modulus is $2.1.10^{11}$N/ m^2.

The experimental directivity of pressure and vibration velocity at 300,1200 Hz and 4600 Hz are given in Fig. 7. At 300 Hz, the theoretical results are almost the same as experimental results. At 1200 Hz, the differences between theoretical and experimental directivity of horizontal vibration velocity begin to grow, but the experimental directivity of pressure and vertical vibration velocity are basically in agreement with theoretical results. At 4600 Hz, the experimental directivity of pressure and horizontal vibration velocity coincides well with theoretical results, while the directivity of vertical vibration velocity deviates seriously from the theoretical directivity. The main reason is that the diffraction wave of the fixture becomes large at high frequency and it will affect the diffraction field of the carrier, thus influencing the measuring results.

Viewing the trend as a whole, the experimental results basically coincide well with the theoretical results, which verify the validity of the computing.

CONCLUSION

Using BEM, the directivity of pressure and vibration velocity of acoustic vector sensor by different carriers is calculated. The conclusions are as follows:

- The influences of diffraction on acoustic vector sensor are proportional to the length of cylinder's radius and height. Besides, the influences from the radius are larger than that from the height. With frequency increasing, the directivity of pressure and vibration velocity becomes worse
- The intensity of diffraction wave concentrates in the *x* axis direction, which makes the directivity of pressure and horizontal vibration velocity less influenced than vertical vibration velocity by the diffraction. When the shape of carrier's undersurface is sharp, the intensity of diffraction wave diffuses all directions and the directivity of acoustic vector sensor is close to natural free field directivity
- Experiment was carried out and the results coincide well with the theoretical results at low frequencies, while at high frequency the diffraction of the fixture will affect the experimental results.

REFERENCES

He, Z.Y. and Y.F. Zhao, 1992. Theoretical Foundation of Acoustics [M]. National Defense Press, pp: 231-237.

Ji, J., G. Liang, Y. Wang and W. Lin, 2010. Influences of prolate spheroidal baffle of sound diffraction on spatial directivity of acoustic vector sensor. Sci. China Technol. Sci., 53(10): 2846-2852.

Kang, K., 2002. Investigation of an underwater acoustic intensity vector sensor. Ph.D. Thesis, Department of Acoustics, the Pennsylvania State University.

Liu, T., J. Fan and W.L. Tang, 2002. Resonance radiation of elastic cylindrical shell in water [J]. Acta Acoust., 27(1): 62-66.

Malcolm, H. and N. Arye, 2000. Acoustic vector-sensor processing in the presence of a reflecting boundary. IEEE T. Signal Proces., 48(11): 2981-2993.

Шендеров., Z. He and J. Zhao, 1983. Wave Propagation Problems of Underwater Acoustics [M]. National Defense Industry Press, pp: 1-5.

Sun, G.Q. and Q.H. Li, 2004. Progress of study on acoustic vector sensor [J]. Acta Acust., 29(6): 481-490.

Tang, W.L. and J. Fan, 2000. Resonance radiation theory of a submerged elastic spherical shell [J]. Acta Acoust., 25(4): 308-312.

Zhuo, L.K., J. Fan and W.L. Tang, 2009. Analyzing acoustic scattering of elastic objects using coupled FEM-BEM technique [J]. J. Shanghai Traffic Univ., 43(8): 1258-1261.